ZEBRAFISH
Volume 8, Number 4, 2011

DOI: 10.1089/zeb.2011.0713



# A Developmental Staging Table for *Astyanax mexicanus* Surface Fish and Pachón Cavefish

Hélène Hinaux,[1] Karen Pottin,[1] Houssein Chalhoub,[1] Stéphane Père,[1] Yannick Elipot,[1] Laurent Legendre,[2] and Sylvie Rétaux[1]

## Abstract

Every model species requires its own developmental table. *Astyanax mexicanus*, a teleost fish comprising both sighted river and blind cave populations, is becoming more and more important in the field of developmental and evolutionary biology. As such, a developmental staging table is increasingly necessary, particularly since comparative analysis of early developmental events is widely employed by researchers. We collected freshly spawned embryos from surface fish and Pachón cavefish populations. Embryos were imaged every 10–12 min during the first day of development, and less frequently in the following days. The results provide an illustrated comparison of selected developmental stages from one cell to hatching of these two populations. The two morphs show an essentially synchronous development regarding major events such as epiboly, neurulation, somitogenesis, heart beating, or hatching. We also present data on particular morphological characters appearing during larval development, such as eye size, yolk regression, swim bladder, and fin development. Some details about the development of F1 Pachón cave×surface hybrids are also given. Comparisons are made with *Danio rerio* (zebrafish) development.

## Introduction

The study of any model organism is greatly enriched by the availability of a developmental staging table.[1–3] This is particularly true for developmental and evolutionary biology studies, as it allows an accurate comparison of different species or populations.

*Astyanax mexicanus*, also previously called *Astyanax fasciatus*, is a teleost fish, belonging to the Ostariophysi group, the same group as the zebrafish *Danio rerio*. However, *Astyanax* is a characiform while *Danio* is a cypriniform, these two lineages having diverged between 100 and 250 million years ago[4,5] (Fig. 1). First described by de Filippi,[6] *Astyanax mexicanus* is widely distributed and endemic to the rivers of Central and South America. Several populations of cave morphs have a very restricted distribution to 29 caves in the region of the Sierra de El Abra in Mexico.[7]

*Astyanax* is increasingly employed as an evo-devo model system.[8,9] Indeed, two types of populations, namely sighted and pigmented river-dwelling populations and blind and unpigmented cave populations, all deriving from surface fish ancestors, are powerful tools for evolutionary biology. The cave forms have diverged at least one million years ago from eyed ancestors, and have evolved specific morphological, neurological, and behavioral traits, allowing their adaptation to the cave environment, characterized by permanent darkness and food scarcity.[10] Surface and cave forms are still inter-fertile and their cross produces a fertile progeny. A comparative study of the surface and cave forms reveals mechanisms of micro-evolution. Furthermore, at least three independent colonization events are at the origin of the 29 known cave populations,[11,12] permitting the study of parallel evolution.[13]

Pachón has been the most commonly used cave population, particularly in evo-devo studies. The transparency of *Astyanax mexicanus* embryos, as well as the fact that abundant spawning can be obtained regularly, facilitates these developmental studies. The synchronous development of Pachón and surface embryos has been hypothesized,[14–20] but never precisely assessed, and no developmental staging table exists for this species. The purpose of this study is to describe and analyze certain developmental details of surface and Pachón fish embryos from the one-cell stage to hatching, and to gain some insights into larval development in these two populations as well as in F1 hybrids.

## Materials and Methods

Laboratory stocks of *A. mexicanus* surface fish and Pachón cave fish were obtained in 2004 from the Jeffery laboratory at

[1]UPR 3294 N&D Laboratory, DECA Group, and [2]GIS AMAGEN CNRS INRA, Institut Alfred Fessard, Gif-sur-Yvette, France.

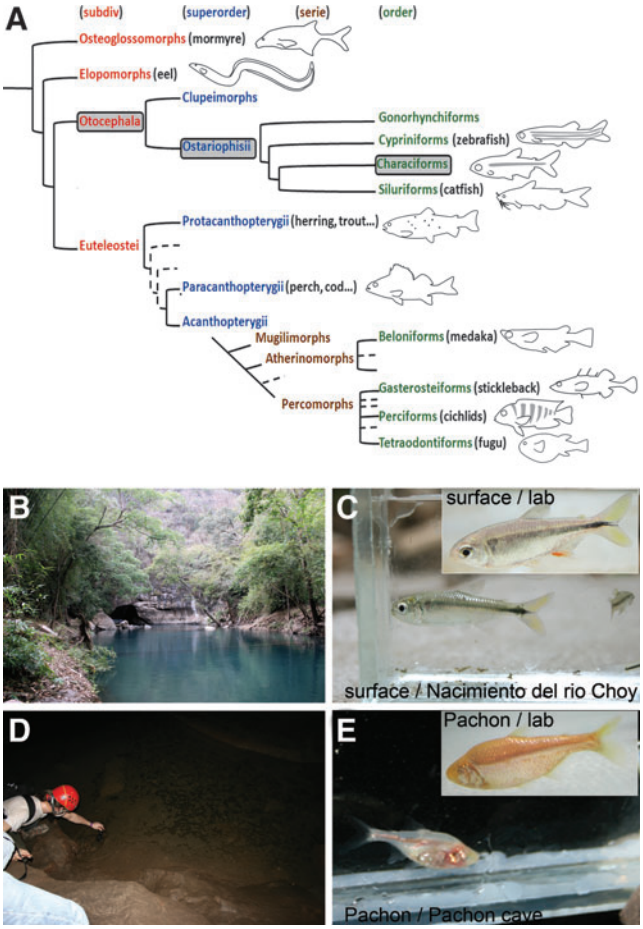


**FIG. 1.** Presentation of *Astyanax mexicanus* model fish. **(A)** Simplified phylogeny of the teleosts, showing *Astyanax mexicanus* positioned among the Characiforms. **(B)** Example of the habitat of the surface form of *Astyanax mexicanus*, in Nacimiento del Rio Choy. **(C)** *Astyanax mexicanus* surface morphs, caught in the wild and a lab specimen (*inset*). **(D)** Pachón cave habitat. **(E)** *Astyanax mexicanus* Pachón cave morphs, caught in Pachón cave and a lab specimen (*inset*).

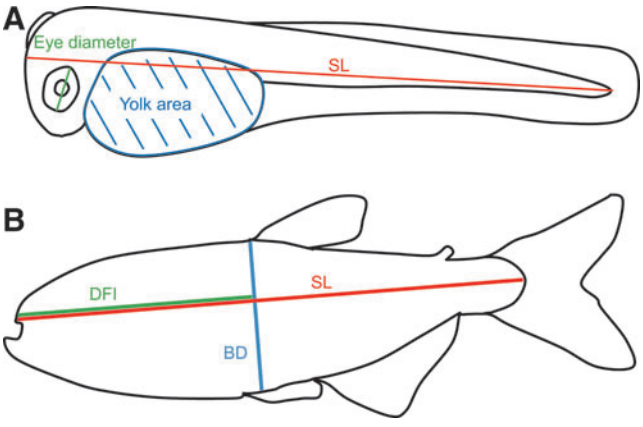


**FIG. 2.** Methods for fish measurements. **(A)** Measurements performed on larvae. **(B)** Measurements performed on adults. BD, body depth; DFI, dorsal fin insertion; SL, standard length.

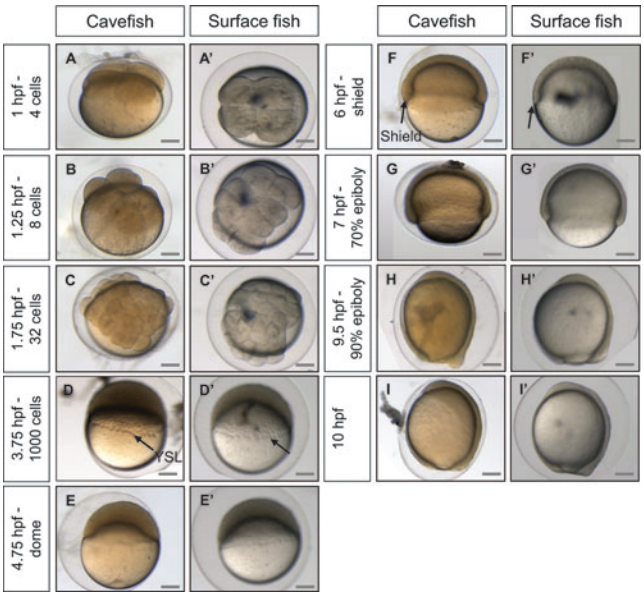


**FIG. 3.** Development of *Astyanax mexicanus* embryos from zero to 10 hpf. Pictures of cavefish **(A–I)** and surface fish **(A′–I′)** embryos at stages indicated on the *left*, views are lateral, except for **A–C′** (views from the animal pole). *Arrows* indicate the yolk syncytial layer (YSL) in **D–D′** and the embryonic shield in **F–F′**. The scale bars represent 200 $\mu$m.

the University of Maryland, College Park, MD. They had been both lab-raised for some generations, and surface fish had initially been collected in San Solomon Spring, Balmorhea State Park, Texas.

In our facility, they were maintained and bred at 23°C (Pachón) and 26°C (surface) on a 12:12 hours light/dark cycle in tap water (pH 8.1–8.2, conductivity 470–590 $\mu$S/cm). These conditions are not too different from the natural environment of these fish (water in Pachón cave: 23.3°C, pH 6.9; water in Nacimiento del Rio Choy: 26°C, pH 7, conductivity 1200 $\mu$S/cm; measurements done in March 2009 and March 2011). Surface × Pachón F1 hybrids were obtained by cohabitation of a female Pachón fish and a male surface fish.

Fish are fed twice a day, once with live food (mosquito worms, artemias) and once with dry food. Surface fish receive TetraMin floating flakes (complete food for all ornamental fish, Tetra) as they feed at the water surface, and cave fish receive TetraPrima Discus sinking granules (complete food for Discus and big ornamental fish, Tetra) as they are bottom feeders. Spawning is induced by changing tank water and shifting temperature (−4°C for surface fish, +4°C for cavefish). It usually occurs in the middle of the night (between midnight and 2:00 AM). Embryos and larvae are maintained in a 23°C incubator in "blue water" (0.017 *M* NaCl, $4.02.10^{-4}$ *M* KCl, $2.72.10^{-4}$ *M* $CaCl_2$, $6.5.10^{-4}$ *M* $MgSO_4$, methylene blue) for 3–4 weeks, and then transferred to "nurseries" in the main fish facility.

For the establishment of the developmental staging table, freshly spawned embryos were collected and imaged every 10–15 min using an Olympus SZX16 stereomicroscope in a room maintained at 23°C. To facilitate somite counts, the chorion of some embryos was removed. Newly hatched larvae were photographed once or twice a day. Pictures of some details of

the larvae were taken using an Apotome microscope (Zeiss). Adult fish were photographed using a Pentax X70 camera.

Standard length (length from snout to caudal fin peduncle), yolk size, eye size, and dorsal fin placement (projection of snout to dorsal fin-length divided by standard length) were measured using ImageJ software. Details of anatomical measurements performed on larvae and adults are depicted in Figure 2. Lengths of the embryos for yolk regression analysis were calculated by extrapolating embryos to a circle, calculating the circumference of this circle and subtracting the head-to-tail straight line length.

Paper chromatography was performed using Whatman paper as the stationary phase and a hexane:benzene 40:60 solution as the solvent. Fresh samples were squeezed against the paper. Spinach leaves were used as reference for pigment separation.

## Results and Discussion

### *Embryonic development*

The development of surface and Pachón embryos was monitored every 10–15 min at 23°C. *Astyanax* embryos are surrounded by a soft chorion like that in *Danio*. However, the *Astyanax* chorion is sticky, leading to the formation of egg clusters, as in Medaka. Segmentation proceeds approximately at the same pace as in *Danio rerio,* with one division every 15 min from the 2-cell stage (Fig. 3). The 1000-cell stage, characterized by the appearance of the yolk syncytial layer (YSL), is reached at 3.75 hpf. Gastrulation proceeds through epiboly and the embryonic shield is visible at 6 hpf, which corresponds to 50% epiboly. Epiboly is completed around

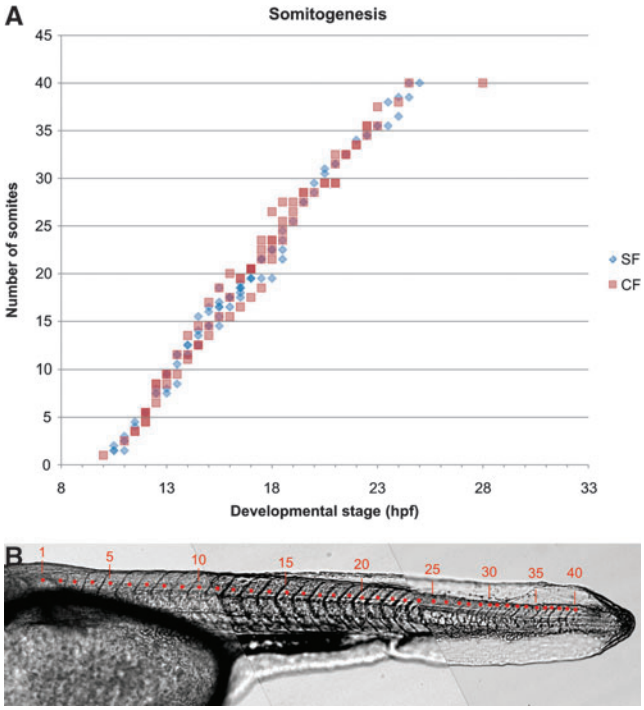


**FIG. 5.** Somitogenesis. **(A)** Timing of somitogenesis in surface and cave embryos as a function of developmental stage. **(B)** Picture showing the definitive number of somites in a 30 hpf surface larva. Each *red dot* indicates one somite. SF means surface fish (*blue*), and CF means cave fish (*red*), as in all following figures.

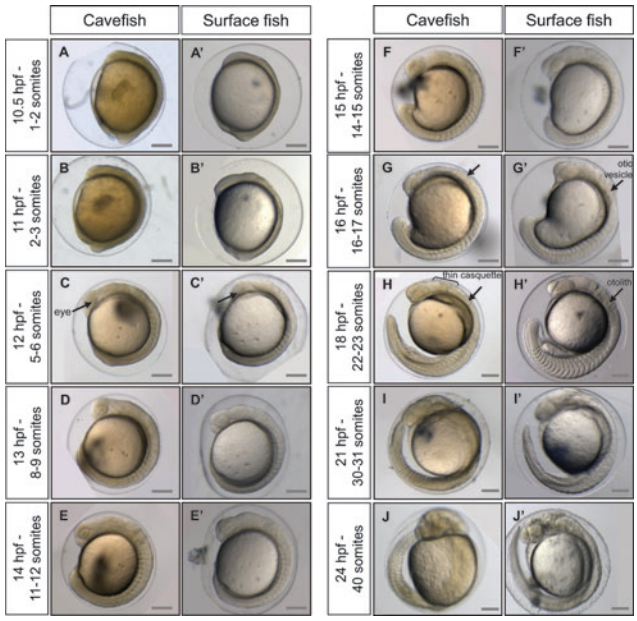


**FIG. 4.** Development of *Astyanax mexicanus* embryos from 10 hpf to 24 hpf. Pictures of cavefish **(A–J)** and surface fish **(A′–J′)** embryos in lateral views, at stages indicated on the *left side. Arrows* in **C–C′** indicate the eye, in **G–G′** the otic vesicle, in **H–H′** an otolith. The *bracket* in **H** indicates the forming casquette, an adhesive gland on the head of the larvae. The scale bars represent 200 $\mu$m.

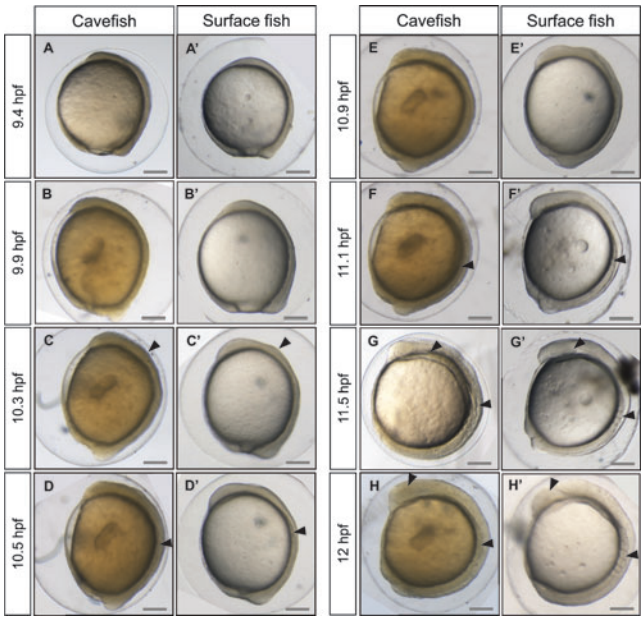


**FIG. 6.** Morphogenetic events during neurulation. Pictures of cavefish **(A–H)** and surface fish **(A′–H′)** embryos in lateral views, with exact stages indicated on the *left. Arrowheads* in **C–C′** and **D–D′** point to comparable shapes and curvatures of the anterior neural plate. *Arrowheads* in **F–F′** indicate the first appearing somites. In **G–G′** and **H–H′** *arrowheads* indicate the somites and the forming eye. The scale bars represent 200 $\mu$m.

Table 1. Main Developmental Landmarks in *Astyanax mexicanus* Development, Compared to *Danio rerio*

| *Astyanax (23°C)* | *Developmental Landmarks* | *Zebrafish (28.5°)* |
|---|---|---|
| 0 hpf | 1-cell stage | 0 hpf |
| 0.75 hpf | 2-cell stage | 0.75 hpf |
| 1 hpf | 4-cell stage | 1 hpf |
| 1.25 hpf | 8-cell stage | 1.25 hpf |
| 1.5 hpf | 16-cell stage | 1.5 hpf |
| 1.75 hpf | 32-cell stage | 1.75 hpf |
| 2 hpf | 64-cell stage | 2 hpf |
| 3.75 hpg | 1000-cell stage (YSL) | 3 hpf |
| 6 hpf | Shield formation | 6 hpf |
| 10.5 hpf | Beginning of somitogenesis | 10.33 hpf |
| 12 hpf | Eye formation | 12 hpf |
| 14 hpf | Otic vesicle becomes visible | 19 hpf |
| 15.5 hpf | Otic vesicle with central depression | |
| 16 hpf | Early motility (first muscle contraction) | 36 hpf |
| 18 hpf | Otolith development | 22 hpf |
| 18 hpf | Very thin casquette becomes visible | |
| 18.5 hpf | Lens becomes visible | 19 hpf |
| 21 hpf | Heart beat; early pigmentation | 24 hpf |
| 24 hpf | End of somitogenesis | 25 hpf |
| 24.5–28 hpf | Hatching | 48 hpf |
| 1.5 dpf–2.7 mm SL | Pectoral fin bud | 42 hpf |
| 3.5 dpf–4 mm SL | Jaws formation | 60 hpf–3.4 mm SL |
| 4.5 dpf–4 mm SL | Casquette disappearance | 3.5 mm SL |
| | Formation of swim bladder | |
| 4–5 mm SL | Yolk complete regression | 6.5 mm SL |
| 5–6 mm SL | Caudal fin ray appearance | 4.9 mm SL |
| 5.5 dpf–3.9 mm SL | Inflated swim bladder | 3.7 mm SL |
| 6–7 mm SL | Anal fin ray appearance | 6.3 mm SL |
| 8.5 mm SL | Adipose fin bud appearance | |
| 8.5 mm SL | Pelvic fin bud appearance | 7.5 mm SL |

10.5 hpf, a time which also corresponds to the appearance of the first somite (Fig. 4). Somitogenesis proceeds synchronously in the two populations (Figs. 4 and 5), with one pair of somites added every 20 min. Neurulation begins between 9.6 and 9.9 hpf, with a visible thickening of the anterior neural plate (Fig. 6). All subsequent developmental milestones are also synchronous in the two populations (Table 1). The eye starts developing at 12 hpf, when 5–6 somites are visible. The otic vesicle becomes visible around 13–14 hpf (8–12 ss), and a central depression is dug at 16–17 hpf (16–12 ss). Around the same time, the embryo starts moving with uncontrolled contractions in the chorion. The tail starts detaching from the yolk and is completely free from any yolk streak around 23 hpf. The casquette, a transient adhesive gland located on the head of the young larvae,[17] becomes visible as a very thin ectodermal thickening at 18 hpf. The lens is visible half an hour later. The heart starts beating around 21 hpf. The larvae hatch between 24.5 and 28 hpf (Fig. 4, Table 1).

*Astyanax* embryonic development at 23°C therefore strongly resembles that of *Danio rerio* at 28.5°C,[2] but is significantly quicker from 12 hpf onwards. Its development is even faster at 28°C. Indeed, at 28°C embryos progress from shield to bud stage in 2.5 h, which normally takes 4 h at 23°C (data not shown). However, at this temperature the survival rate is low, and as such, 23°C appears to be the ideal temperature at which to maintain embryos. Surface and Pachón cavefish embryos have a completely synchronous development until hatching. The early development of Pachón × surface hybrid embryos is synchronous as well (Supplementary Fig. S1; Supplementary data are available online at www.liebertonline.com/zeb). The only difference between the two types of embryos is with respect to pigmentation: Pachón embryos remain unpigmented, whereas the eye and yolk of surface fish embryos start showing pigment cells (black melanophores) between 19 and 23 hpf (Fig. 4, Table 1).

Another intriguing variation between these embryos is the color of the yolk from spawning time: surface embryos are completely transparent, whereas Pachón embryos are slightly orange while remaining translucent (Fig. 3). We hypothesized that this difference could stem from feeding differences in breeding adults in our facility (see Methods). We performed paper chromatography of cave and surface food jointly with spinach extracts used as a reference (Supplementary Fig. S2). This analysis showed that adult cavefish food contains carotenes while surface fish food does not. Thus, the orange coloration of the cavefish yolk could be the result of carotene reserves. Paper chromatography of cave and surface egg extracts showed that cave eggs contain xanthophylles, raising the possibility that cave females oxygenate carotenes from their food and incorporate the resulting xanthophylles into their eggs (Supplementary Fig. S2). This would explain why hybrid embryos also appear yellowish (Supplementary Fig. S1), as the mother of these hybrids is a Pachón cavefish.

### *Larval development*

After hatching, *Astyanax* larvae are first twisted but then straighten within half an hour. They possess 40 somites, the definitive number being reached at 25 hpf (Figs. 5 and 7Bb). Zebrafish on the other hand reach 30–32 somites at 25 hpf and hatch at 48 hpf.[2,21] Most *Astyanax* sensory organs are functional upon hatching: the otic vesicle is well developed with 2 otoliths (appeared at 18 hpf (Fig. 4)), the casquette is smooth and sticky (Fig. 7Aa), the lateral line primordium can be seen along the larva body (Fig. 7Ab), nostrils are open (Fig. 7Ba), the lens and retina are clearly recognizable (Fig. 7Bd), with the ventral quadrants missing or reduced in cave larvae (Fig. 7Ac).[16] Certain other structures can be documented: the cloaca is formed (Fig. 7Ae) but the rest of the digestive tract cannot be recognized. A pectoral fin bud can be seen along the yolk (Fig. 7Ad). Cells of the notochord are round and do not overlap (Fig. 7Bc). Skin differentiation is nearly complete: keratinocytes aggregate in the caudal fin (Fig. 7Af) and mucus cells can be seen in the epidermis (Figs. 7Be and 7Bf).

Half a day later at 2 dpf (Figs. 7C and 7D), larvae have grown (2.7 to 3.5 mm standard length), as has the pectoral fin

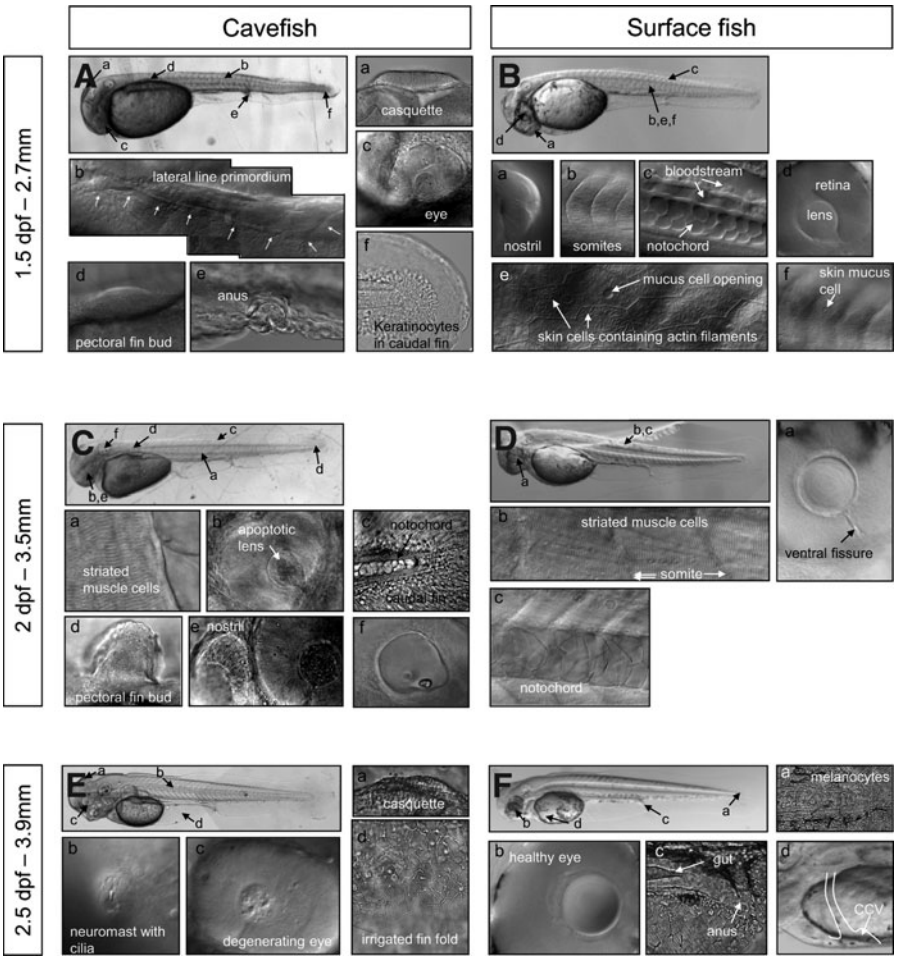


**FIG. 7.** Early larval development. Cavefish **(A, C, E)** and surface fish **(B, D, F)** embryos in lateral views, at 1.5 dpf **(A, B)**, 2 dpf **(C, D)**, and 2.5 dpf **(E, F)**. In all images, anterior is *left* and dorsal is *up*. Images of anatomical details are shown and located on the global view, and captions are written in full on the pictures. CCV stands for common cardinal vein, also called duct of Cuvier.

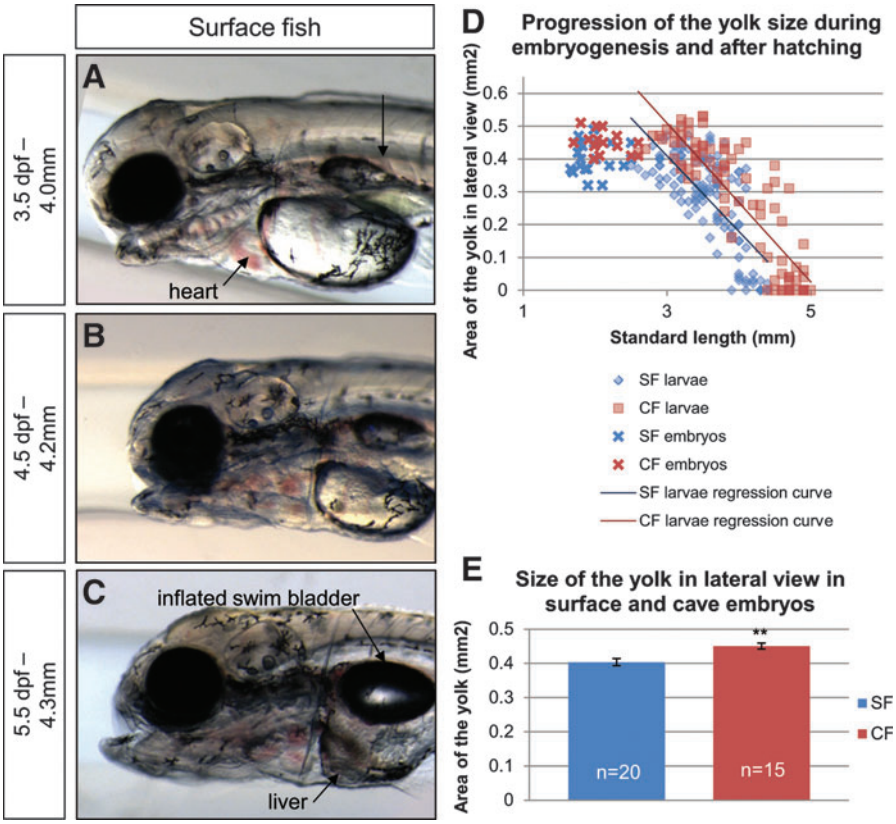


**FIG. 8.** Yolk regression during the first days of larval life. **(A–C)** Surface fish larvae in lateral view at 3.5 dpf, 4.5 dpf, and 5.5 dpf. The black arrow in **A** indicates the forming swim bladder. **(D)** Quantification of the yolk size and its progressive disappearance, as seen in lateral view, in surface (*blue symbols*) and cave (*red symbols*) embryos and larvae. **(E)** Mean size of the yolk in surface and cave embryos from 10 to 20 hpf. Statistical significance was calculated using Mann-Whitney test.

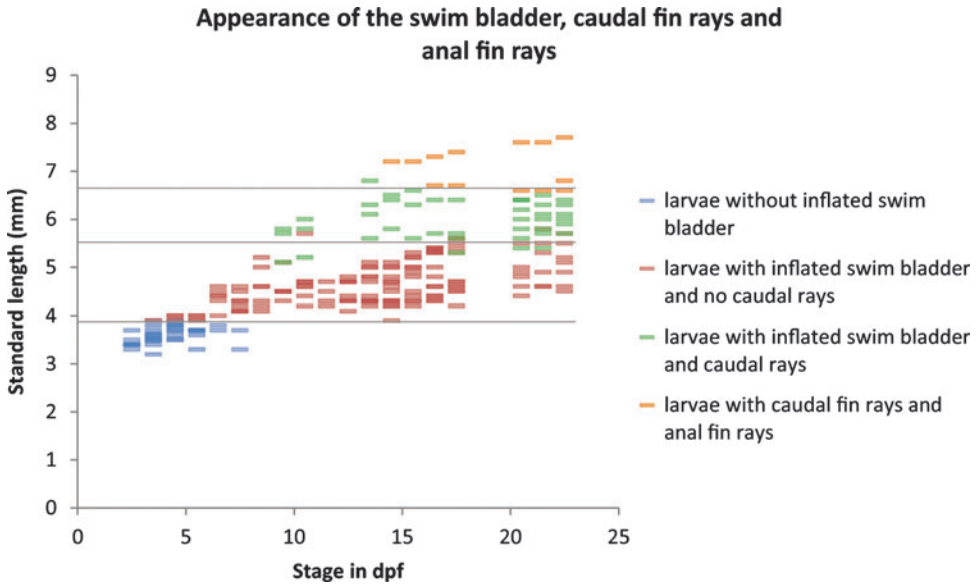


**FIG. 9.** Standard length-dependence of certain larval characteristics. Surface fish larvae reared at 23°C or 28°C and at different population densities (from 5 to 150 per 60 mm dish) were assessed for the appearance of certain larval characteristics and reported as a function of age (*x-axis*) and SL (*y-axis*) during 3 weeks. Colors indicate swim bladder inflation (*red*), appearance of caudal (*green*), and anal (*orange*) fin rays, as indicated on the *right*.

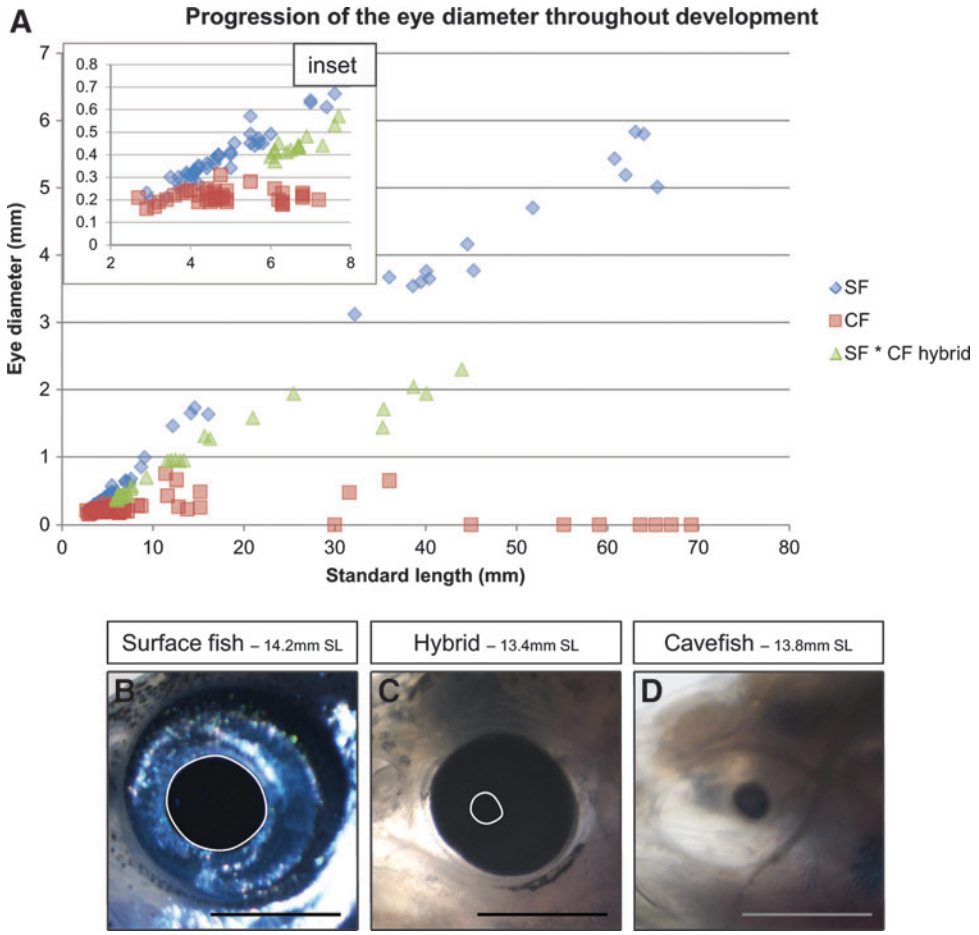


**FIG. 10.** Eye size during development. **(A)** Quantification of eye diameter in surface (*blue*), cave (*red*), and F1 hybrid (*green*) larvae, as a function of standard length. The *inset* shows a magnification of the measures for early embryos. **(B–D)** Pictures of the eye of equally sized surface **(B),** hybrid **(C),** and cave **(D)** fishes. *Solid lines* outline the lens. In cavefish, the degenerated eye appears slightly dark because it is a cyst of high density, which makes it difficult for the transmitted light to cross. The scale bar represents 1 mm.

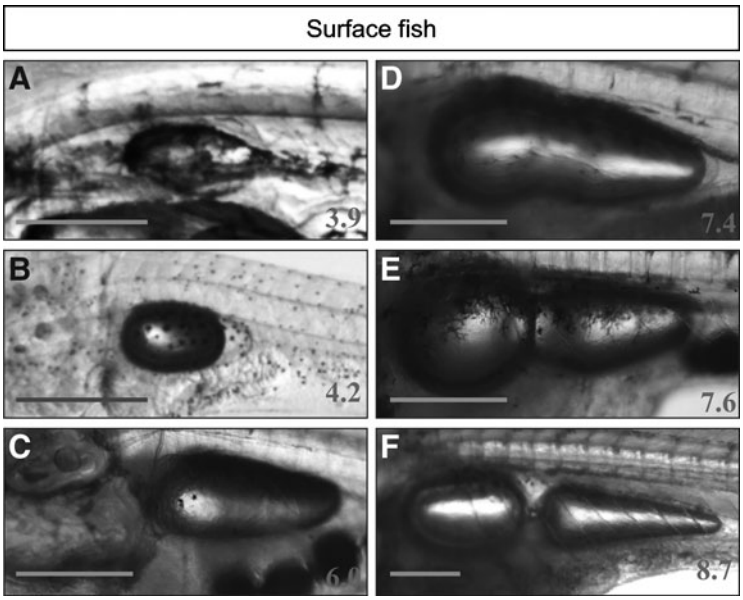


**FIG. 11.** Swim bladder development. **(A–F)** Pictures of surface fish larvae in lateral views, with the anterior side on the *left*. Their standard lengths (SL) are indicated on the bottom right corner of the pictures. The scale bar represents 500 $\mu$m.

bud (Fig. 7Cd). The cells of the notochord are bigger, overlapping, and polygonal in shape (Figs. 7Cc and 7Dc). Striated muscle cells are clearly visible (Figs. 7Ca and 7Db). Blood appears clearly red in vessels (not shown but see Fig. 8). The apoptotic lens of the cave larvae appears rippled (Figs. 7Cb and 7Ce), in contrast with the smooth and healthy lens of surface larvae (Fig. 7Da).

At 2.5 dpf (Figs. 7E and 7F), larvae begin to develop jaws. Neuromasts with their cilia can be observed along the lateral line (Fig. 7Eb). The casquette is usually bumpier than at 1.5 dpf (Fig. 7Ea). In the cavefish degenerating eye, the lens is barely recognizable (Figs. 7Ec and 7Fb). The digestive tract is almost complete (Fig. 7Fc). In surface fish, star-shaped melanocytes can be seen in the skin (Fig. 7Fa). The vitelline blood circulation of the larvae strikingly resembles that of zebrafish but not medaka,[22,23] with a single common cardinal vein on the yolk (Fig. 7Fd, Supplementary Video SV1; Supplementary Video is available on www.liebertpub.com/zeb).

At 3.5 dpf, the casquette is completely degenerated (Fig. 8A). The swim bladder becomes visible as a deflated pouch (Fig. 8A). It will inflate only at 5.5 dpf, when the digestive tract is complete and larvae start feeding. At this time the yolk, which has progressively reduced since hatching, has mostly disappeared (Figs. 8A–8C). Yolk regression proceeds linearly from hatching, until complete disappearance when larvae reach 4.5–5 mm standard length (Fig. 8D). Cave embryos possess a slightly larger yolk and use it at the same rate as surface larvae, so that yolk disappears later in cave larvae (Figs. 8D and 8E). This confirms previous reports of bigger eggs in subterranean *Astyanax*.[24,25]

The larger the larvae become, the more their growth and development depends on the space they occupy and the density of the population in which they are reared. For instance, a 2-month-old larva can measure from 6 to 20 mm, depending on the water volume, the population density, the temperature, and the amount of food available. The definitive adult size (6–7 cm) is reached within 1 to 3 years. Most characteristics depend on the standard length (SL) of larvae rather than their age. For example, the swim bladder inflation can occur between 3.5 and 7.5 dpf, but is always achieved at 3.9 mm SL (Fig. 9, red dots). The appearance of caudal fin rays and anal fin rays also depends on standard length (Fig. 9, green and orange dots, respectively). Thus, the relevant measure to stage the larvae is the standard length, and not the age, as in zebrafish.[26] In all of the following figures, observed characteristics will therefore be analyzed as a function of the standard length.

### *Eye development*

One major difference between surface and cave adult fish is the presence or absence of an eye. The degeneration of the cavefish eye was monitored throughout larval development to adulthood, by measuring the diameter of the eyes of surface, Pachón cave and F1 hybrid larvae, and young adults (Figs. 2 and 10A). Cavefish eyes undergo almost normal morphogenesis (see also Fig. 4) and grow during the first days of larval development, but the eye diameter never exceeds 0.3 mm (Fig. 10A inset), and eventually decreases to zero. In contrast, surface fish eyes undergo continuous growth until adulthood. F1 hybrid eyes also grow until adulthood, but at all stages they are smaller than surface fish eyes, as previously shown.[27] For illustration, pictures of surface, cave, and hybrid eyes of approximately 14 mm SL larvae are shown (Figs. 10B–10D).

### *Swim bladder development*

The swim bladder develops the same way in surface, cave, and hybrid larvae. At approximately 4 mm SL it inflates, and then grows antero-posteriorly (Figs. 9 and 11). A bud appears anteriorly when the larvae reach about 7 mm SL and gives rise to the anterior swim bladder. Around 8.5 mm SL, anterior and posterior swim bladders are connected only by a thin tube, as in adults. This is the same type of development as seen in *Danio rerio*, even if corresponding standard lengths differ,[26] as adult zebrafish are much smaller than *Astyanax mexicanus*.

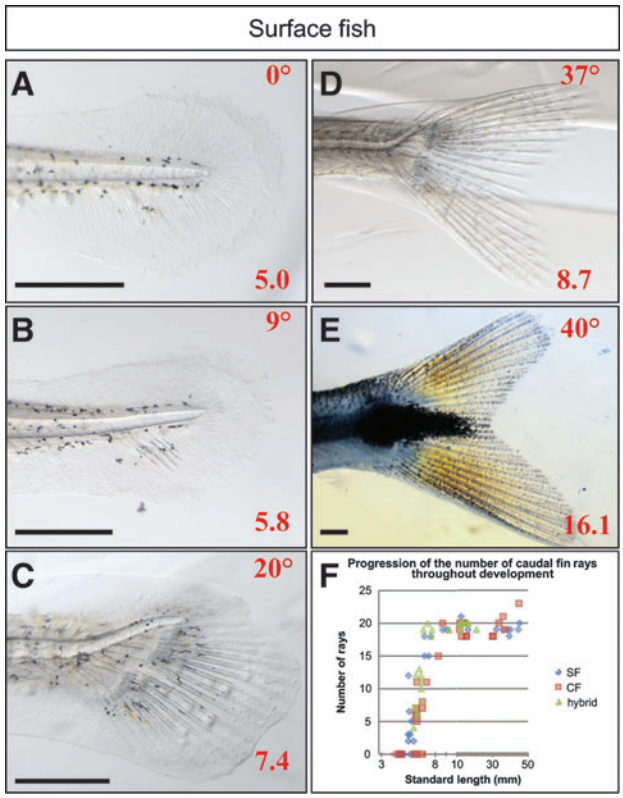


*Fin development*

The caudal fin is the first to develop, with the first rays appearing around 5 mm SL (Fig. 12). The notochord progressively bends dorsally so that the spine is found finally only in the dorsal part of the fin. The definitive number of rays (20 rays, with some inter-individual variation observed) is reached at 9 mm SL in all populations (Fig. 12G). Hybrid and surface larvae develop the same way, with pigmentation appearing progressively: first, a central black melanophore spot together with melanophores between the rays; and then, xanthophores appear on the entire fin (Figs. 12A–12F). In contrast, cave fish are never pigmented but development of the fin structure as a function of length follows the same time course as surface and hybrid larvae.

The anal fin appears at 7 mm SL. Cave fish were reported to possess fewer anal fin rays as adults than surface fish,[28] which

**FIG. 12.** Caudal fin development. **(A–E)** Surface fish larvae caudal fins in lateral views, with standard lengths indicated at the *bottom right* of each picture. The bending angle of the notochord is indicated in the *top right corner* of each picture. The scale bars represent 500 $\mu$m. **(F)** Quantification of the number of caudal fin rays as a function of standard length in surface (*blue*), hybrid (*green*), and cavefish (*red*).

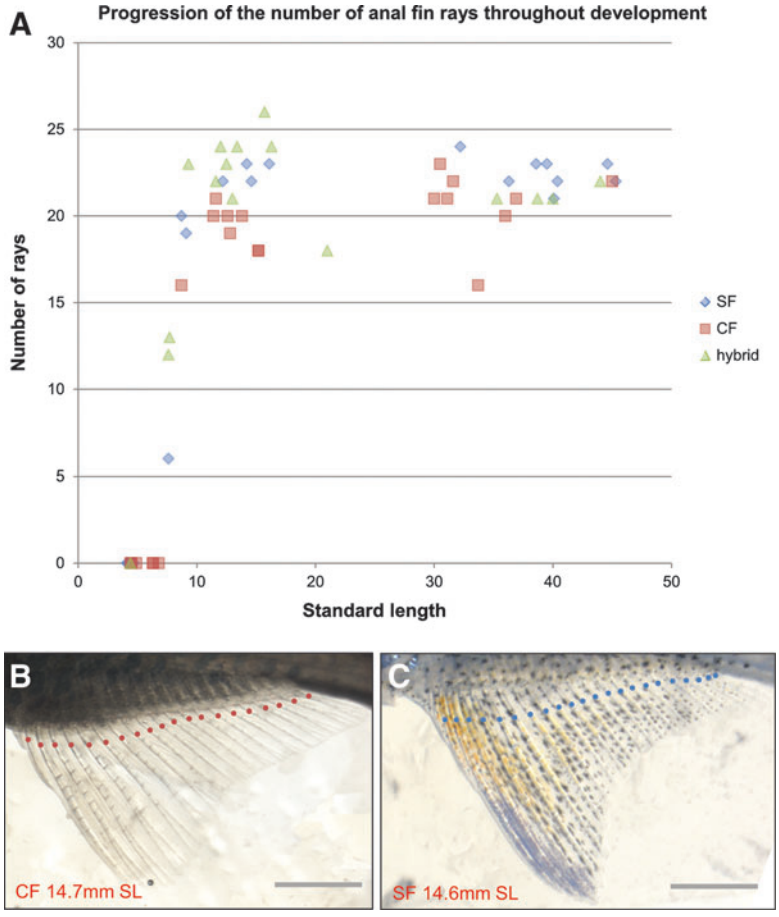


**FIG. 13.** Anal fin development. **(A)** Quantification of the number of anal fin rays as a function of standard length in surface, hybrid, and cavefish. **(B)** Cavefish anal fin, with *red dots* indicating the rays. **(C)** Surface fish anal fin, with *blue dots* indicating rays. The scale bars represent 1 mm.

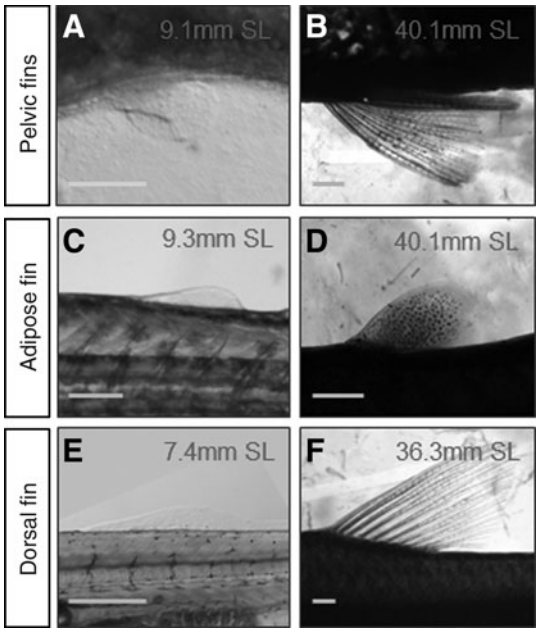


is why we analyzed anal fin ray number throughout development. The definitive number of anal fin rays is reached at 15 mm SL approximately (around 23 rays), and is indeed slightly lower in cave fish (around 20 rays) (Fig. 13). Similarly F1 hybrids tend to have only 20 rays.

The pelvic fin buds appear at 9 mm SL, and rays are formed at 11.5 mm SL (Figs. 14A and 14B). The adipose fin, a fleshy fin located posteriorly to the dorsal fin, also appears as a bud at 9 mm SL and remains without rays (Figs. 14C and 14D). This special type of fin can be found in characids but also in lizardfishes (Synodontidae), Siluriforms, and salmonids (Salmonidae).[29,30] Finally, the dorsal fin, consisting of 10 or 11 rays, first appears at 8 mm SL and all rays are present around 10mm SL (Figs. 14E and 14F).

**FIG. 14.** Pelvic, adipose, and dorsal fin development. Pictures of pelvic fins **(A, B)**, adipose fins **(C, D)**, and dorsal fins **(E, F)** in surface fish of various standard lengths. The scale bars represent 250 $\mu$m in **A, C, E,** and 1 mm in **B, D, F.**

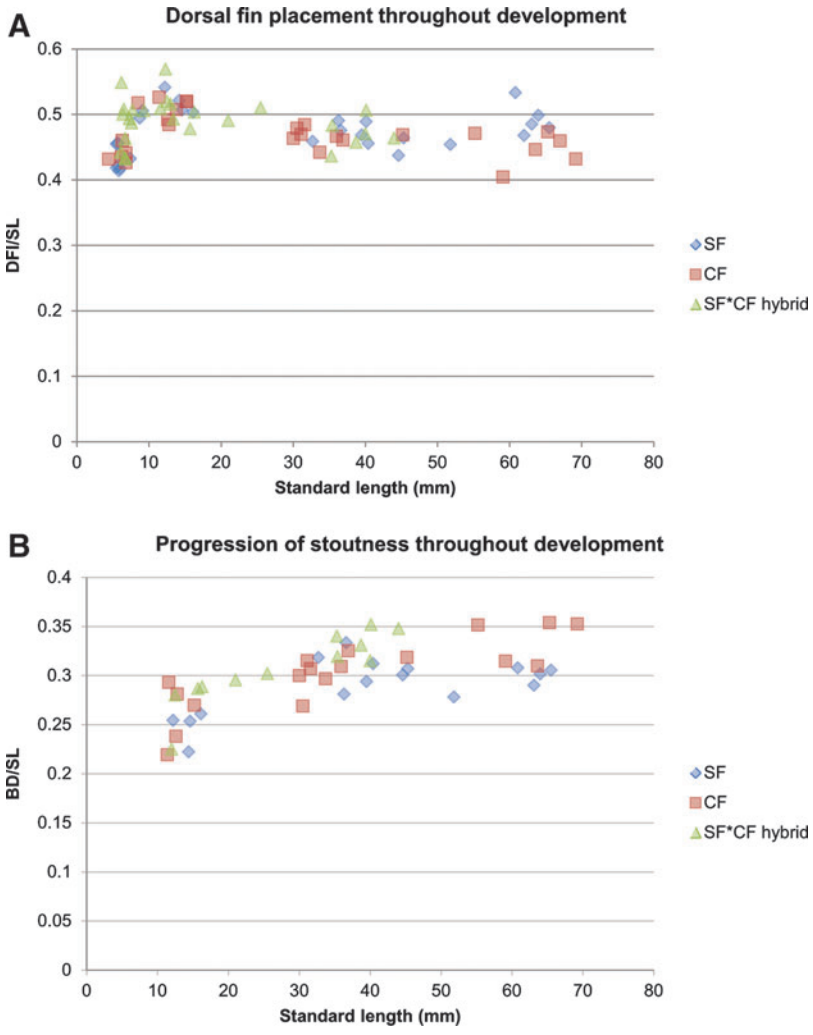


**FIG. 15.** Global body shape. **(A)** Quantification of the placement of the dorsal fin along the body axis (see Fig. 2 for Methods) as a function of the standard length. **(B)** Quantification of body stoutness as a function of the standard length. For adult specimens (above 40 mm SL), the values are always higher for cavefish.

### *Development of global body shape*

The dorsal fin has previously been reported to be positioned more posteriorly in Pachón fish than in surface fish.[28] We measured its placement throughout development but were unable to confirm this observation: our data, obtained with projection on the body axis to correct for differences in corpulence between the two populations (Fig. 2) show identical dorsal fin placement in surface, Pachón cave, and F1 hybrid fishes (Fig. 15A). We also quantified stoutness (body depth divided by SL, Fig. 2). As expected from general observations and from the fact that Pachón are fatter than surface fish (at least in laboratory conditions), for individuals with SL above 40 mm, Pachón fish were more corpulent than surface fish (Fig. 15B). Thus, the QTL reported by Protas et al. (2008) may be related to a difference in growth and global body shape, rather than to a difference in dorsal fin placement in cavefish.

## Conclusion

*Astyanax mexicanus* embryonic development is very fast: a swimming larva hatches one day after fertilization at 23°C. Embryos and early larvae are totally transparent, allowing for live imaging as well as high quality molecular histology. Surface fish and Pachón cavefish embryos and larvae exhibit a strictly synchronous development, allowing rigorous comparisons between these two populations both during embryogenesis and in later development. In the laboratory, embryos and larvae of each population are nevertheless easily recognizable by the color and shape of early embryos, the presence or absence of pigmentation, and the morphology of the eye. Some very slight variations between individuals can sometimes be observed, mostly in cavefish. During development, somitogenesis proceeds with some interindividual variation (Fig. 5), and cavefish embryos are globally more variable than surface fish embryos. This is also true for the eye development (Fig. 10) and for all molecular markers studied so far. On the other hand, adults within a single population differ only in gender-dependent body shape (females have a rounder belly than males), and, for surface fish, by pigmentation influenced by the social status (dominant individuals have more intense orange spots on the anal fin). Together with the facts that 1) *Astyanax* is easy to propagate and regularly provides a large number of embryos, 2) surface and cave fishes can breed and allow genetic approaches, and 3) the evolutionary history of the different populations is known, the developmental features we have described here contribute to the making of *Astyanax mexicanus* an excellent model for evolutionary developmental biology, as well as for developmental biology *per se*. The current limitations of the model for transcriptomics, genomics, and transgenesis should also be overcome in the very near future.

## Acknowledgments

Work supported by an ANR grant (ASTYCO) to SR. Thanks to Philippe Herbomel with whom we "traveled" through *Astyanax* larvae under Nomarski optics at the early stages of the project. We also wish to thank Matthieu Simion and the animal facility staff for help and advice in fish care, and Heather McLean for improvement of our English.

## Disclosure Statement

No competing financial interests exist.

## References

1. Iwamatsu T. Stages of normal development in the medaka *Oryzias latipes*. Mech Develop 2004;121:605–618.
2. Kimmel CB, Ballard WW, Kimmel SR, Ullmann B, Schilling TF. Stages of embryonic development of the zebrafish. Dev Dyn 1995;203:253–310.
3. Swarup H. Stages in the development of the stickleback *Gasterosteus aculeatus* (L.). J Embryol Exp Morph 1958;6:373–383.
4. Briggs JC. The biogeography of otophysan fishes (*Ostariophysi:Otophysi*): A new appraisal. J Biogeogr 2005;32: 287–294.
5. Peng Z, He S, Wang J, Wang W, Diogo R. Mitochondrial molecular clocks and the origin of the major Otocephalan clades (Pisces: Teleostei): A new insight. Gene 2006;370:113–124.
6. De Filippi F. Nouvelles espèces de poissons. Revue Magasin Zoologie. 1853; (Serie 2) volume 5: 164–171.
7. Mitchell RW, Russell WH, Elliott WR. Mexican eyeless characin fishes, genus Astyanax: Environment, distribution, and evolution. Spec Publ Mus Texas Tech Univ 1977;12:1–89.
8. Jeffery WR. Cavefish as a model system in evolutionary developmental biology. Dev Biol 2001;231:1–12.
9. Jeffery WR. Emerging model systems in evo-devo: Cavefish and microevolution of development. Evol Dev 2008;10: 265–272.
10. Wilkens H. Evolution and genetics of epigean and cave *Astyanax fasciatus* (Characidae, Pisces). Support for the neutral mutation theory. In: Hecht, MK, Wallace, B (Eds) Evolutionary Biology vol 23 Plenum, New York and London. 1988:271–367.
11. Strecker U, Bernatchez L, Wilkens H. Genetic divergence between cave and surface populations of Astyanax in Mexico (Characidae, Teleostei). Mol Ecol 2003;12:699–710.
12. Strecker U, Faundez VH, Wilkens H. Phylogeography of surface and cave Astyanax (Teleostei) from Central and North America based on cytochrome b sequence data. Mol Phylogen Evol 2004;33:469–481.
13. Jeffery W. Regressive evolution in Astyanax cavefish. Ann Rev Gen 2009 43:25–47.
14. Alunni A, Menuet A, Candal E, Penigault JB, Jeffery WR, Retaux S. Developmental mechanisms for retinal degeneration in the blind cavefish *Astyanax mexicanus*. J Comp Neurol 2007;505:221–233.
15. Menuet A, Alunni A, Joly JS, Jeffery WR, Retaux S: Expanded expression of Sonic Hedgehog in *Astyanax* cavefish: Multiple consequences on forebrain development and evolution. Development 2007;134:845–855.
16. Pottin K, Hinaux H, Retaux S: Restoring eye size in *Astyanax mexicanus* blind cavefish embryos through modulation of the Shh and Fgf8 forebrain organising centres. Development 2011;138:2467–2476.
17. Pottin K, Hyacinthe C, Retaux S. Conservation, development, and function of a cement gland-like structure in the fish *Astyanax mexicanus*. Proc Natl Acad Sci USA 2010;107: 17256–17261.
18. Yamamoto Y, Byerly MS, Jackman WR, Jeffery WR. Pleiotropic functions of embryonic sonic hedgehog expression link jaw and taste bud amplification with eye loss during cavefish evolution. Dev Biol 2009;330:200–211.
19. Yamamoto Y, Jeffery WR. Central role for the lens in cave fish eye degeneration. Science 2000;289:631–633.

20. Yamamoto Y, Stock DW, Jeffery WR. Hedgehog signalling controls eye degeneration in blind cavefish. Nature 2004;431: 844–847.
21. Holley SA. The genetics and embryology of zebrafish metamerism. Dev Dyn 2007;236:1422–1449.
22. Fujita M, Isogai S, Kudo A. Vascular anatomy of the developing medaka, *Oryzias latipes*: A complementary fish model for cardiovascular research on vertebrates. Dev Dyn 2006;235:734–746.
23. Isogai S, Horiguchi M, Weinstein BM. The vascular anatomy of the developing zebrafish: An atlas of embryonic and early larval development. Dev Biol 2001;230:278–301.
24. Hüppop K. Phänomene und Bedeutung der Energieersparnis bei dem Höhlenfisch *Astyanax fasciatus* (Characidae, Pisces). Thesis, Universität Hamburg, 1988.
25. Hüppop KaW, H. Bigger eggs in subterranean *Astyanax fasciatus* (Characidae, Pisces). Z zool Syst Evolut 1991;29: 280–288.
26. Parichy DM, Elizondo MR, Mills MG, Gordon TN, Engeszer RE. Normal table of postembryonic zebrafish development: Staging by externally visible anatomy of the living fish. Dev Dyn 2009;238:2975–3015.
27. Borowsky R. Restoring sight in blind cavefish. Curr Biol 2008;18:R23–24.
28. Protas M, Tabansky I, Conrad M, Gross JB, Vidal O, Tabin CJ, et al. Multi-trait evolution in a cave fish, *Astyanax mexicanus*. Evol Dev 2008;10:196–209.
29. Fishbase. http://wwwfishbaseorg/searchphp (last accessed November 2011).
30. Helfman GS, Collette BB, Facey DE, Bowen BW. The diversity of fishes. Biology, evolution, and ecology. Wiley Blackwell publishers. 2009; Second Edition.

Address correspondence to:
*Sylvie Rétaux, Ph.D.*
*UPR 3294 N&D Laboratory*
*Institut de Neurobiologie Alfred Fessard*
*CNRS*
*Avenue de la Terrasse*
*91198 Gif-sur-Yvette cedex*
*France*

*E-mail:* retaux@inaf.cnrs-gif.fr